國立高雄應用科技大學

100-101 年度獎勵科技大學及技術學院教學卓越計畫

產學及研究成果轉專題製作教材

Image White balance based on A Non-diagonal Model

Image White balance based on A Non-diagonal Model

電機工程系 黃敬群教授 學生黃得凱

Abstract

White balance is an algorithm proposed to mimic the color constancy mechanism of human perception. However, as shown by its name, current white balance algorithms only promise to correct the color shift of gray tone to a correct position; for other color values, white balance algorithms process them as gray tone and therefore produce undesired color bias. To improve the color prediction of white balance algorithms, in this paper, we propose a 3-parameter non-diagonal model, named as *PCA-CLSE*, for white balance. Unlike many previous researches which use the von-Kries diagonal model for color prediction, we proposed to apply a non-diagonal model for color correction which aimed to minimize the color biases while keeping the balance of white color. In our method, to reduce the color biases, we proposed a *PCA*-based training method to gain extra information for analysis and built a mapping model between illumination and non-diagonal transformation matrices. While a color-biased image is given, we could estimate the illumination and dynamically determine the illumination-dependent transformation matrix to correct the color-biased image. Our evaluation shows that the proposed *PCA-CLSE* model can efficiently reduce the color biases.

1. PROBLEM STATEMENT

1.1. Von-Kries diagonal model

Von-Kries diagonal model for color prediction from illumination *B* to illumination *A* could be generalized as

$$\begin{bmatrix} R_A \\ G_A \\ B_A \end{bmatrix} = \begin{bmatrix} C_r & 0 & 0 \\ 0 & C_g & 0 \\ 0 & 0 & C_b \end{bmatrix} \begin{bmatrix} R_B \\ G_B \\ B_B \end{bmatrix}, \qquad (1)$$

where (R_A,G_A,B_A) and (R_B,G_B,B_B) are the color vectors of the same surface reflectance under different lighting. The coefficients, C_r, C_g, C_b, on the other hand, define the color ratios of three color channels independently. Here, for the *i*th color channel, the ratio is chosen as the ratio of the *i*th illumination color L_i obtained from a white surface under the two illuminations *A* and *B*:

$$C_i = \frac{L_i^{A,white}}{L_i^{B,white}}. \qquad (2)$$

In principle, von-Kries model assumes the ratios, C_r, C_g, C_b, which are used for color correction under the two illuminations, are same as the color ratios of a white surface.

However, the von-Kires diagonal model is not a perfect color prediction model. This can be theoretically understood by considering the formation process of an image. For the image formation, the relation among the color vectors $\mathbf{f}=(R,G,B)^T$, the illumination spectrum $e(\lambda)$, the surface spectral reflectance function $r(\lambda)$, and the sensor sensitivity function $s_i(\lambda)$ of the *i*th color channel is represented as

$$f_i = \int_\omega e(\lambda) r(\lambda) s_i(\lambda) d\lambda, \qquad (3)$$

where λ indicates spectrum and the integral is taken over the visible spectrum ω. Next, the ratio of the *i*th color response of a surface under two illuminations is then calculated by

$$\frac{f_i^A}{f_i^B} = \frac{\int_\omega e^A(\lambda) r(\lambda) s_i(\lambda) d\lambda}{\int_\omega e^B(\lambda) r(\lambda) s_i(\lambda) d\lambda}. \qquad (4)$$

In general, $r(\lambda)$ could not be pull out from the integral and could not be cancelled. That is

$$\frac{f_i^A}{f_i^B} \neq \frac{\int_\omega e^A(\lambda) s_i(\lambda) d\lambda}{\int_\omega e^B(\lambda) s_i(\lambda) d\lambda} \frac{L_i^{A,white}}{L_i^{B,white}} = C_i. \qquad (5)$$

Therefore, the color ratio is not a constant for different surfaces with different colors and von Kries diagonal model only can only work as an approximation for color prediction. Note that in (5), we define the illumination colors L_i^{white} as the response of the *i*th color channel of a white surface. This is same as the definition used in [3].

Sometimes, von-Kries diagonal model may work well with some kinds of sensors, especially for those sensors with very sharp sensitivities. This could be easily understood based on (4). While the sensor has an extremely narrow-band sensitivity function, for example the Dirac delta function, $r(\lambda)$ could be pull out from the integral and the color ratio in (4) become a constant for different surfaces. Under

the condition, the von-Kries diagonal model becomes applicable.

However, as reported by Finlayson et al. [6], the von-Kries diagonal model could not provide accurate color prediction in most cases and the approximation may produce significant color biases. To overcome the problem, Barnard et al. proposed the sensor sharpening method in [7], which maps the color responses into a new color space where the sensor is sharper by a fixed linear transform *T*. The main technique issue in sensor sharpening is how to find the optimal linear transform *T*. Focusing on this issue, in [8], Xiao et al. discussed the preferred color spaces for white balance.

Even though the sensor sharpening method could be applied to improve the accuracy of color prediction, the optimal transform *T* for sensor sharpening is pre-learned and illumination-independent. In this paper, we find the color biases, which are the difference between the true colors and the predicted colors, are dependent on illumination. Instead of applying a fixed linear transform *T*, we look for an illumination-adaptive transform to dynamically correct the color biases.

1.2. Color biases

In this section, we use an experiment to understand how color biases or color prediction errors happen if the von- Kries model is used. To conduct the experiment, we use the Simon Fraser University color dataset [9], which contains 287 different illumination spectrums, 1995 surface reflectance functions, and 3 sensor sensitivity functions for different color channels.

In the experiment, to demonstrate the color biases, we randomly select illumination spectrums and 24 surface reflectance functions from the color dataset. By using the sensor sensitivity functions to measure the color responses by equation (3), we could synthesize our standard images. A standard image has 24 grids under a uniform illumination. In Figure 1(a) and 1(b) we show two standard images under illumination *A* and illumination *B* separately. Note that the 24 surface patches used in the two standard images are same in order to demonstrate the color difference caused by the environmental lighting. Next, we use the von-Kries model to predict the color change from illumination *B* to illumination *A*. Assume we could correctly estimate the illumination colors $L_i^{A,white}$ and $L_i^{B,white}$, the coefficients, C_r, C_g, C_b, of the von-Krie diagonal model could be determined by equation (2). In Figure 1(c), we could see the color correction result by using the diagonal model As we can see, Figure 1(a) and Figure 1(c) have close color appearance and the color difference caused by the environmental lighting is greatly removed.

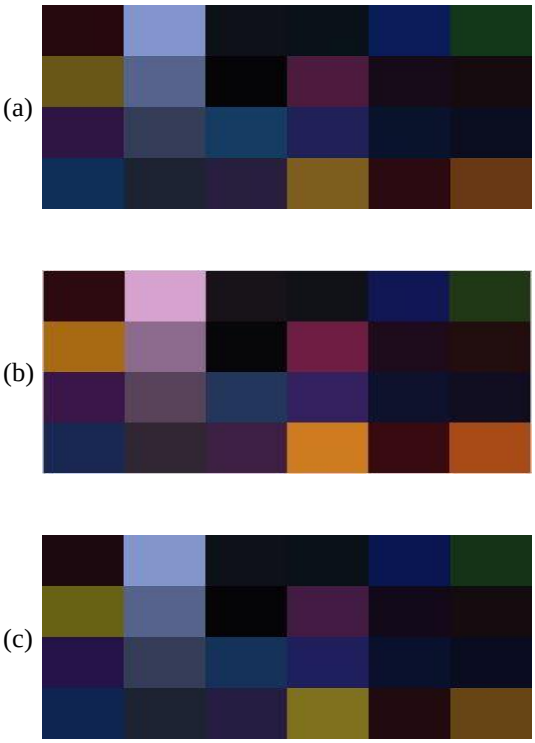

Fig. 1: The standard images (a) under illuminate *A* and (b) under illuminate *B*. (c) The color correction result from illumination *B* to illumination *A* based on von-Kries model.

However, we could also find that there exist color biases, or say prediction error, between Figure 1(a) and Figure 1(c). For example, the yellow color at the bottom row. To measure the color difference, we use the angular error (***AE***) between the predicted color vector $\vec{\boldsymbol{P}}$ and the true color vector $\vec{\boldsymbol{T}}$. That is

$$AE = \cos^{-1}(\vec{\boldsymbol{P}} \cdot \vec{\boldsymbol{T}}). \quad (6)$$

In Table 1, the angular errors between Figure 1(a) and 1(c) are listed for reference. Therefore, how to reduce the color biases becomes our system goal. In this paper, we proposed a new method to dynamically reduce the prediction error based on the estimation of illumination and a learning process.

Table 1: Angular errors between the true colors and the colors predicted by the von-Kries diagonal model for the tested images in Figure 1.

8.6093^0	0.2248^0	0.0203^0	1.6505^0	2.8694^0	3.1326^0
3.4104^0	0.0325^0	0.1920^0	5.0963^0	8.4276^0	2.4559^0
8.2998^0	0.0237^0	2.5548^0	2.6343^0	2.8203^0	1.9361^0
2.9233^0	0.0958^0	2.7688^0	5.4492^0	6.3184^0	5.2911^0

2. WHITE BALANCE BASED ON A NON-DIAGONAL MODEL

In this paper, we proposed a non-diagonal model for white balance. Here, to improve the accuracy of the von-Kries diagonal model for color prediction, we proposed to use a full 3x3 non-diagonal transformation matrix as a replacement. The non-diagonal model has more degrees of freedom and hence would be more accurate. However, it is difficult to determine the 9 parameters of the non-diagonal model due to the lack of information. In general, only 3 degrees of freedom could be determined if the illumination information is available. To overcome the problem, the proposed system relied on an offline learning process to gain extra information. The basic idea is to train and record the correspondence between environmental illumination and its optimal transformation matrix in an efficient manner. While the illumination is estimated, we could dynamically determine the transformation matrix from the trained model. Hence, even thought we only have illumination information for 3 degrees of freedom, we could also adopt a non-diagonal model to boost the accuracy.

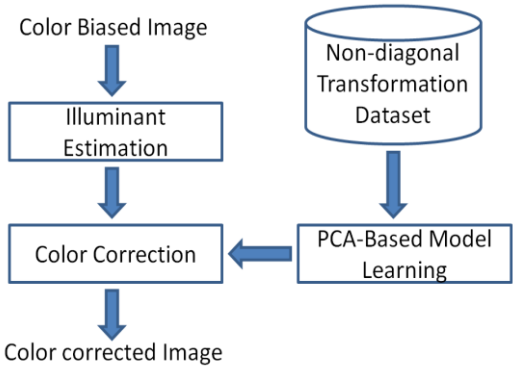

Fig. 2: The system flow of the proposed white balance method based on a non-diagonal color prediction model.

The system flow of the proposed method is shown in the Figure 2, which is composed of a testing phase and a learning phase. In the testing phase, our system estimates the color of the environmental illumination. With illumination estimation, a transformation matrix is selected from the offline learned model for color correction. In the learning phase, lots of transformation matrices under various lighting condition are collected for training. In our system, we find the transformation matrices collected for training play a crucial step. In this paper, we proposed a new method for sample collection to replace the conventional method proposed in [4]. With the proposed method, we ensure the training samples are specific selected for white balance. Hence, the trained model is more accurate. To train the model, *PCA* is utilized to extract a compact subspace of transformation matrix. This learned subspace provides a systematic way to record the mapping between the environmental illumination and its optimal non-diagonal transformation and forms the trained model. Below, we describe the each step of our system in detail.

2.1. Illumination estimation

Illumination estimation is an important step toward white balance. To estimate the color of illumination, some assumptions should be made. Until now, most of systems use the gray-world hypothesis or the gray-edge hypothesis for illumination estimation. In this paper, we use both methods to estimate illumination in our experiments. Below we explain the estimation process separately.

2.1.1. Gray-world hypothesis

In [10], the author proposed the grey-world hypothesis. For gray-world hypothesis, the basic assumption is that the average of reflectance in the scene is achromatic. This could be expressed as

$$\frac{\int r(\lambda, x)dx}{\int dx} = k. \qquad (7)$$

In (7), k is some constant and $r(\lambda, x)$ is the spectrum response of the reflectance at location x. If a color image is denoted as $f(x)$, the intensity average of the ith color channel over the spatial coordinate could be calculated by

$$\frac{\int f_i(x)\,dx}{\int dx} = \frac{1}{\int dx}\int\int_{\omega} e(\lambda)r(\lambda,x)s_i(\lambda)\,d\lambda\,dx$$

$$= \int_{\omega}\left[\int \frac{r(\lambda,x)}{\int dx}dx\right]e(\lambda)s_i(\lambda)\,d\lambda = k\cdot L_i \qquad .(8)$$

Here, $i \in \{r,g,b\}$ and L_i is the illumination color of the ith color channel as before. Form (8), the illumination color L_i could be estimated by

averaging the given image $f(x)$.

Recently, the authors in [11] proposed a generalized formulation for white balance on the Minkowski norm. In their formulation, the illumination color is computed by

$$k \cdot L_i = \left(\frac{\int f_i^{\,p}(x)\,dx}{\int dx} \right)^{\frac{1}{p}}. \qquad (9)$$

It could be found that if p=1, the equation is equal to the gray-world assumption.

2.1.2. Gray-edge hypothesis

As an alternative to the gray-world hypothesis, Weijer and Gevers [12] propose the gray-edge hypothesis. The fundamental assumption is that the average derivative of the reflectance of surfaces is achromatic. Note that the derivative could be interpreted as the edge intensity. Based on the assumption, we have

$$\frac{\int |r_x(\lambda, x)|\,dx}{\int dx} = k \cdot \qquad (10)$$

In (10), the subscript **x** indicates the spatial derivative. If the spatial derivative of a color image is denoted as $f_x(x)$, the average derivative intensity of the ith color channel over the spatial coordinate is given by

$$\frac{\int |f_{x,i}(x)|dx}{\int dx} = \frac{1}{\int dx} \int \int_{\omega} e(\lambda)\,|r_x(\lambda, x)|\,s_i(\lambda)\,d\lambda\,dx$$
$$= \int_{\omega} \left[\int \frac{|r_x(\lambda, x)|}{\int dx} dx \right] e(\lambda) s_i(\lambda)\,d\lambda = k \cdot L_i \qquad .(11)$$

Therefore, based on the gray-edge assumption, the illumination color L_i could be estimated by averaging the derivative intensity of the given image $f_x(x)$. As the gray-world hypothesis, the generalized gray-edge hypothesis on the Minkowski norm is represented as

$$k \cdot L_i = \left(\frac{\int |f_{x,i}(x)|^p dx}{\int dx} \right)^{\frac{1}{p}}. \qquad (12)$$

2.2. PCA-based model learning

A non-diagonal 3x3 transformation matrix M_{BA} for color prediction from illumination B to illumination A could be expressed as

$$\begin{bmatrix} R_A \\ G_A \\ B_A \end{bmatrix} = \begin{bmatrix} C_{11} & C_{12} & C_{13} \\ C_{21} & C_{22} & C_{23} \\ C_{31} & C_{32} & C_{33} \end{bmatrix} \begin{bmatrix} R_B \\ G_B \\ B_B \end{bmatrix} = M_{BA} \begin{bmatrix} R_B \\ G_B \\ B_B \end{bmatrix}, \qquad (13)$$

where (R_A,G_A,B_A) and (R_B,G_B,B_B) are the color vector of the same surface reflectance under two different lighting. To find the optimal transformation matrix, there are 9 parameters of M_{BA} to be determined. As known from the previous section, illumination estimation provides only 3-parameter information. In order to use the full 3x3 model, we look for learning methods to extract information from training datasets.

Among the previous works, we found the method proposed by Funt and Jiang [4] is applicable. In [4], the authors proposed to use principle component analysis (PCA) to analyze the 3x3 linear transformations that model illumination change. In detail, if we reshape a 3x3 matrix as a vector, each matrix is represented by a point in a 9-dimensional space. Since the transformation matrix is independent on the object reflectance and only models the illumination change, a reasonable hypothesis used in [4] is to assume that the underlying distribution of all possible transformation matrices are embedded in a 3-dimensional subspace. To verify the hypothesis and learn the 3-dimensional subspace, *PCA* is applied to analyze the space of the transformation matrix. One major difference between the proposed method and the method in [4] is how to collect proper transformation matrices for *PCA*. To be clear, we will detail the difference in section 3.4.

In our system, we collect N transformation matrices into a training set $\{M_i\}_{i=1\sim N}$. Suppose M_0 is the mean matrix of the training set $\{M_i\}_{i=1\sim N}$. By subtracting the mean matrix M_0 and rearranging the N matrices into a N-by-9 data matrix, we get a data matrix D_m, with zero empirical mean, for principle component analysis. Here, each row of D_m indicates the 9 elements of a 3-by-3 transformation matrix after subtracting M_0. Next, we calculate the covariance matrix of D_m and denote it as C_m. After finding the eigenvectors and eigenvalues of C_m, we may find most of the training samples are compactly concentrated in a 3-dimentional subspace.

To build the learning model for the selection of illumination transformation, the three eigenvectors with the top 3 eigenvalues are chose. By reshaping the three eigenvectors back

to 3-by-3 matrices, we finally obtain three basis matrices Z_1, Z_2, and Z_3. The set $\mathbf{Z}=\{Z_1,Z_2,Z_3\}$ and the mean matrix M_0 form a compact subspace of the illumination transformation matrix. We then defined the subspace as the trained model. With the model, each illumination transformation matrix M could be well approximated by

$$M \approx a_1 Z_1 + a_2 Z_2 + a_3 Z_3 + M_0 = T(a_1, a_2, a_3; \mathbf{Z}, M_0). \quad (14)$$

That is, the non-diagonal illumination transformation is determined by three parameters $\{a_1,a_2,a_3\}$ instead of 9 parameters. Also in (14), we denote the trained model as $T(a_1,a_2,a_3;\mathbf{Z},M_0)$. With $T(a_1,a_2,a_3;\mathbf{Z},M_0)$, if the estimated illumination of a tested image can provide 3-parameter information to determine $\{a_1,a_2,a_3\}$, the matrix M_{cc} for image color correction could be selected. Therefore, in concept, the model $T(a_1,a_2,a_3;\mathbf{Z},M_0)$ serves as a mapping function between the estimated illumination and the transformation matrix.

2.3. Color correction

Once the illumination is estimated and the model of illumination transformation is learned, our system would dynamically select the optimal transformation matrix for color correction. The policy is to select a transformation matrix to correct the color shift of white patches so that the white balance requirement is met. Therefore, if we denote the estimated illumination of a tested image as $L^t=(L_r,L_g,L_b)$ and the standard white color as $L^w=(255, 255, 2555)$, the color correction matrix we select for white balance should satisfy $L^w=M_{cc}L^t$. With the model $T(a_1,a_2,a_3;\mathbf{Z},M_0)$, we can derive the following equation.

$$\begin{aligned} L^w &= (a_1 Z_1 + a_2 Z_2 + a_3 Z_3 + M_0) L^t \\ &= \begin{bmatrix} Z_1(1)L^t & Z_2(1)L^t & Z_3(1)L^t \\ Z_1(2)L^t & Z_2(2)L^t & Z_3(2)L^t \\ Z_1(3)L^t & Z_2(3)L^t & Z_3(3)L^t \end{bmatrix} \begin{bmatrix} a_1 \\ a_2 \\ a_3 \end{bmatrix} + M_0 L^t. \end{aligned} \quad (15)$$

Here, $Z_i(j)$ indicates the jth row of the basis matrix Z_i. Since the illumination L^t has been estimated, the mean matrix M_0 have been determined, and the basis matrix Z_i have been learned, the three parameters $\{a_1,a_2,a_3\}$ could be directly calculated. With $\{a_1,a_2,a_3\}$ the optimal transformation matrix M_{cc} could be selected. Finally, with the selected M_{cc}, any color pixel of the tested image is corrected by equation (13) in order to obtain the color-corrected image with white balance.

2.4. The collection of training samples

Before this section, we focus on model learning and how to use the trained model for white balance. However, to determine the subspace of illumination transformation, lots of samples of transformation matrices under various illumination pairs should be collected for training. In our system, we found that how to properly select training samples is much important. Without using the training dataset which is specifically collected for white balance, the trained model may be biased. Until now, few relative researches focus on this sample selection issue. Thus, in this paper, for image white balance, we proposed a new method to select training samples

In [4], the author proposed to select the sample of illumination transformation in the least square error (*LSE*) sense. To get a matrix sample of illumination transformation, in their method, they randomly choose two illuminations, named as *A* and *B*, from the Simon Fraser University color dataset. The color responses of 1995 surface reflectance under the two illuminations are measured based on the equation (3) to build two color sets. The optimal transformation matrix $M_{BA,LSE}$ provides the least square mapping error between the two color set is calculated and then selected as one training sample. This could be expressed as

$$M_{BA,LSE} = \arg\min_{M} \sum_{i=1}^{1995} |C_{i,A} - MC_{i,B}|^2 . \quad (16)$$

In (16), $C_{i,j}$ is the ith color vector in the jth color sets. We should note that the optimal transformation matrix $M_{BA,LSE}$ under the least square error constraints does not make $C_{i,A}=M_{BA}C_{i,B}$ for any color vector pair but provide a best compromise solution among all color vector pairs.

However, for the application of white balance, the sample selection policy in [4] should be further modified. Essentially, the method is not suitable for white balance. To explain the reason, we consider the color correction step in our system. The important goal is to dynamically determine the transformation matrix based on the illumination color L^t, the canonical illumination color L^w, and the white balance constraint $L^w=M_{cc}L^t$. However, the optimal least-square-error solution $M_{tw,LSE}$, which is the ideal matrix we prefer to select, does not meet the white balance constraint. That is $L^w \neq M_{tw,LSE}L^t$. Therefore, the matrix M_{cc} we select for color correction is away from the ideal solution $M_{tw,LSE}$. Hence, the sample selection

policy in [4] should be further modified.

In this paper, to modify the selection method, we redefine the ideal matrix for illumination transformation. Here, instead of minimizing the color prediction error for all color vectors, an ideal transformation matrix in our definition should minimize the color prediction error and satisfy the white balance requirement. With this definition, we proposed to select the transformation sample from illuminations A to illuminations B by using a constrained least square error (*CLSE*), defined as

$$M_{BA,CLSE} = \arg\min_{M} \sum_{i=1}^{1995} |C_{i,A} - MC_{i,B}|^2 . \quad (17)$$
$$\text{subject to } L^A = ML^B$$

In (17), L^A and L^B are the color vectors of illuminations A and B. Here, to solve this constrained optimization problem, we use the Lagrange multiplier method [13].

Next, We collect a training set $\{M_{i,CLSE}\}_{i=1\sim N}$ in the *CLSE* sense and apply PCA to analyze the embedded subspace. By verifying the eigenvalues, we find that most samples within the training set could be 99% approximated by using three eigenvectors. Based on this result, we could ideally assume that the suitable color correction matrix for illumination transformation from any B to A is within a learnable 3-dimensional subspace. Since the matrices inside this new model attempt to make $L^B=M_{BA,CLSE}L^A$, we could apply the white balance constraint to select the transformation matrix inside the new model with less model selection error.

3. SYSTEM SUMMARIZATION

3.1. System implementation

The implementation steps of the proposed system are summarized as follows.

(1) The learning phase:
   A. Collect N training samples $\{M_i\}_{i=1\sim N}$ in the *CLSE* sense defined in (17).
   B. Apply PCA to the training sample set $\{M_i\}_{i=1\sim N}$ and learn the illumination transformation model $T_{CLSE}(a_1,a_2,a_3;\mathbf{Z},M_0)$.

(2) The testing phase:
   A. Given a color-biased image, we estimate the color vector L^t of illumination based on the gray-world hypothesis by using (9) or based on the gray-edge hypothesis by using (12).
   B. According the estimated illumination L^t and the trained model $T_{CLSE}(a_1,a_2,a_3;\mathbf{Z},M_0)$, we calculate the three parameters $\{a_1,a_2,a_3\}$ by using (15) and determine the color correction matrix $M_{cc,CLSE}$ by using (14).
   C. With $M_{cc,CLSE}$, the color vector of each pixel in the tested image is corrected by equation (13) in order to obtain the color-corrected image.

3.2 Symbol Notation

In Table 2, we summary the symbols used in the paper.

Table 2: Symbol Notation.

Symbol	Description
$M_{BA,LSE}$	The optimal *LSE* color correction matrix for illumination pair (A,B).
$M_{BA,CLSE}$	The optimal *CLSE* color correction matrix for illumination pair (A,B)..
T_{LSE}	The *LSE* 3-dimensional matrix model
T_{CLSE}	The *CLSE* 3-dimensional matrix model
$M_{cc,LSE}$	The color correction matrix selected from T_{LSE} based on the white balance constraint.
$M_{cc,CLSE}$	The color correction matrix selected from T_{CLSE} based on the white balance constraint.
$M_{cc,diag}$	The von-Kries diagonal color correction matrix.

4. EXPERIMENTS

In our experiment, the data is from the Simon Fraser University color dataset [9], which contains 287 different illumination spectrums and 1995 surface reflectance functions. Our experiments have three parts. In the first part, we verify that the distribution of color correction transformation matrices is roughly embedded in a 3-dimensional subspace. In the second part, we evaluate the performance of three color prediction models, including the von-Kries model $M_{cc,diag}$, the *PCA-LSE* non-diagonal model $M_{cc,LSE}$, and the *PCA-CLSE* non-diagonal model $M_{cc,CLSE}$. Here, to be discriminative, *PCA-LSE* and *PCA-CLSE* are used to represent *PCA* with *LSE* samples and *CLSE* samples correspondingly. In the third part, we demonstrate the performance of white balance based on the three color prediction models by using many color-biased images.

4.1 Verification of Three-Dimension Hypothesis

In this subsection, we verify the hypothesis that both the distribution of *LSE* matrix samples and the distribution of *CLSE* matrix samples could be well approximated by 3-dimensional subspaces. Note the two subspaces are different.

Here, we present the covered data energy as a function of the dimension number of the *PC*A model in the Figure 3. As we could see from the figure, for both the *PCA-LSE* and *PCA-CLSE* cases, onlt three main eigenvectors are enough to cover more than 99% data energy of the training dataset.

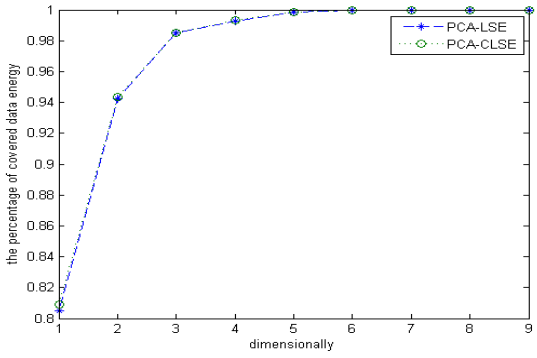

Fig. 3: The percentage of covered data energy as a function of the dimension number of the *PCA* model.

4.2 Model Comparison

To evaluate the performance of a color prediction model M, we use the color dataset [9] to synthesize color sets $\{C_{i,A}\}$ and $\{C_{i,B}\}$ under an illumination pair (A,B). Each set has 1995 color response vectors. The performance of M is then determined by measuring the average L2 norm error. That is

$$E\_M = \sum_{i=1}^{1995} |C_{i,A} - MC_{i,B}|^2 \,/1995. \qquad (18)$$

In (18), E_M indicates the error of model. In our experiments, we compare the performance of matrices $M_{BA,LSE}$, $M_{BA,CLSE}$, $M_{cc,LSE}$, $M_{cc,CLSE}$, and $M_{cc,diag}$. It should be noted that only $M_{cc,LSE}$, $M_{cc,CLSE}$, and $M_{cc,diag}$ could be determined and used in the testing phase. However, the performance of $M_{BA,LSE}$ and $M_{BA,CLSE}$ could serve as the optimal solution bounds for performance evaluation.

Basically, in least square error sense, $M_{BA,LSE}$ is the optimal solution. If we add the illumination constraint $L^B=ML^A$ as an extra condition, $M_{BA,CLSE}$ becomes the best solution. In Table 3, we provide the color prediction performance of different transformation matrices. In our experiments, we have tested more than 300 illumination pairs though only the details of 9 illumination pairs are reported in the table. Here, we could find the $M_{BA,LSE}$ is the best solution. However, since we rely on the illumination constraint $L^B=ML^A$ to dynamically select the transformation matrix in the testing phase, the best solution that we could and should approach is $M_{BA,CLSE}$. Note that under the constraint $L^B=ML^A$, $M_{BA,CLSE}$ always outperforms matrices $M_{cc,LSE}$, $M_{cc,CLSE}$, and $M_{cc,diag}$. Also, since $M_{cc,CLSE}$ is selected to approach $M_{BA,CLSE}$, $M_{cc,CLSE}$ has better prediction performance than $M_{cc,LSE}$ and $M_{cc,diag}$. Furthermore, without using the information from learning process, the diagonal model $M_{cc,diag}$ loses some prediction accuracy comparing with $M_{cc,CLSE}$ and $M_{cc,LSE}$.

Table 3: The average L2 norm error of color prediction by using different matrices under different illumination pairs. Here, "Pair_*i*" represents the *i*th illumination pair. "Avg" is the average results of all illumination pairs.

	$E\_M_{BA,LSE}$	$E\_M_{BA,CLSE}$	$E\_M_{cc,LSE}$	$E\_M_{cc,CLSE}$	$E\_M_{cc,diag}$
Pair_1	66.5749	80.9645	88.9434	88.4121	136.5637
Pair_2	92.8401	96.8588	106.0871	105.6406	175.8792
Pair_3	85.3215	88.5303	100.4778	98.4465	128.2589
Pair_4	128.8683	136.1685	151.4551	148.8011	198.7618
Pair_5	45.6411	49.6539	65.8880	63.3145	70.4688
Pair_6	87.9820	115.4584	132.3479	129.7332	176.5549
Pair_7	92.810	120.2660	138.4639	135.5461	184.8110
Pair_8	128.2839	155.3272	168.2428	165.9508	195.8254
Pair_9	73.7972	76.3346	88.1190	87.0840	117.1466
Avg	97.0286	110.115	121.1579	118.9739	157.9720

Furthermore, it is worth to discuss the performance of $M_{cc,LSE}$ and $M_{cc,CLSE}$. In the original design, $M_{cc,LSE}$ is selected to approach the *LSE* optimal solution $M_{BA,LSE}$, while $M_{BA,CLSE}$ is selected to approach the *CLSE* optimal solution $M_{BA,CLSE}$. Here, we define model selection error as the difference between the selected matrix and the target matrix. A major reason that causes the model selection error is the use of 3-dimentional approximation. In general, the optimal solution is close but not inside the trained subspace. The approximation error therefore generates the model selection error. In order to understand the model selection error, in Table 4, we measure the average color prediction difference $M_{\mathrm{Sel}}\_M_{\mathrm{Tar}}$ of the selected matrix M_{Sel} and the target matrix M_{Tar} over 1995 color response vectors. That is

$$M_{Sel}\_M_{Tar} = \sum_{i=1}^{1995} |M_{Sel}C_i - M_{Tar}C_i|^2 \,/1995. \quad (19)$$

In Table 4, we find the model selection error between $M_{cc,CLSE}$ and $M_{BA,CLSE}$ is smaller than the error between $M_{cc,LSE}$ and $M_{BA,LSE}$. This is because, for the *LSE* case, not only the approximation error but also the improper use of the white balance constraint causes the model selection error. In contrast, for the *CLSE* case,

only the approximation error affects the model selection error. If the approximation error goes to zero, the model selection error will approach zero, and $M_{cc,CLSE}$ will almost be equal to $M_{BA,CLSE}$.

Table 4: The model selection error $M_{Sel}\_M_{Tar}$ between the selected matrix M_{Sel} and the target matrix M_{Tar}.

	$M_{cc,LSE}\_M_{BA,LSE}$	$M_{cc,CLSE}\_M_{BA,CLSE}$
Pair_1	22.3685	7.44
Pair_2	13.2470	8.7818
Pair_3	15.1563	9.9162
Pair_4	22.5868	12.6326
Pair_5	20.2469	13.6605
Pair_6	44.3659	14.2748
Pair_7	45.6539	15.2802
Pair_8	39.9589	10.6236
Pair_9	14.3218	10.7494
Avg	24.1293	8.8587

Finally, to compare with the von-Kries model, we test the *PCA-LSE* non-diagonal model and the *PCA-CLSE* non-diagonal model on the color prediction experiment, which is mentioned in the Figure 1 and Table 1. From, Table 1, Table 5, and Table 6, we may find that the *PCA-CLSE* non-diagonal model provides better color prediction in most patches.

Table 5: Angular errors between the true colors and the colors predicted by the *PCA-LSE* non-diagonal model for the tested images in Figure 1.

3.7265°	0.8212°	0.0693°	0.9929°	0.5656°	2.2217°
2.2059°	0.4539°	0.1428°	1.0245°	4.2607°	0.4962°
3.7469°	0.2856°	1.2769°	1.5191°	0.8395°	1.2703°
0.6250°	0.1071°	1.0234°	1.8744°	2.1400°	1.4873°

Table 6: Angular errors between the true colors and the colors predicted by the *PCA-CLSE* non-diagonal model for the tested images in Figure 1.

3.7530°	0.7924°	0.0689°	0.9460°	0.2667°	1.8929°
1.8213°	0.4430°	0.1316°	0.9831°	4.2553°	0.4487°
3.6846°	0.2792°	1.3250°	1.2585°	0.6350°	1.0578°
0.7440°	0.1073°	0.9284°	1.5240°	2.1706	1.1943°

4.3 White Balance Results

In this subsection, we use some color-based images to evaluate the proposed white balance system. For each tested image, we estimate the illumination based on the gray-world hypothesis and the gray-edge hypothesis. The true illumination is also provided for comparison. Next, based on the proposed system, we dynamically select the best *PCA-CLSE* non-diagonal model from the trained model for color correction. In Figure 4 and 5, we show the white balance results. In Table 7, we show the illumination estimation of the two tested images. Here, we may find the accuracy of illumination estimation is highly relative to the system performance.

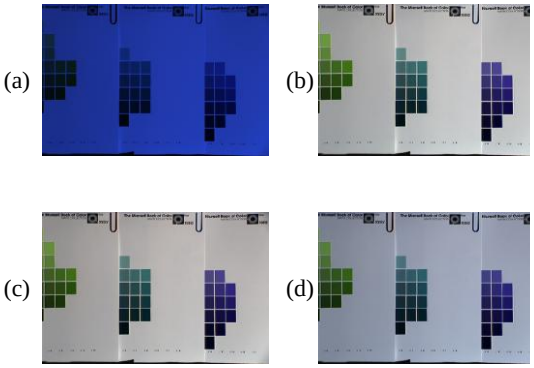

Fig. 4: (a) A color-biased image and its white balance results based on (b) true illumination, (c) gray-world illumination estimation, and (d) gray-edge illumination estimation with *PCA-CLSE* color correction.

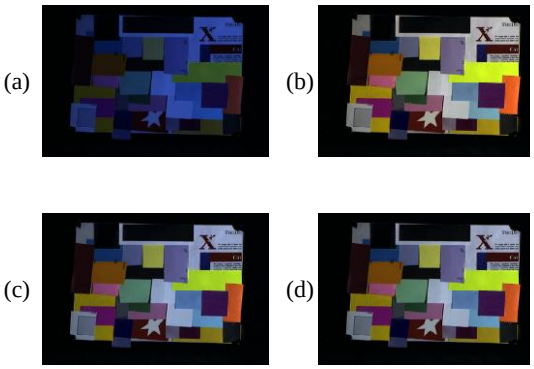

Fig. 5: (a) A color-biased image and its white balance results based on (b) true illumination, (c) gray-world illumination estimation, and (d) gray-edge illumination estimation with *PCA-CLSE* color correction.

Table 7: Illumination estimation based on gray-world (Ill_{GW}) and gray-edge (Ill_{GE}) and their angular errors (AE) comparing with the true illumination (Ill_{True}).

Image	Ill_{True}	Ill_{GW}	Ill_{GE}	AE_{GW}	AE_{GE}
Fig. 4	(0.18,0.31,0.93)	(0.17,0.31,0.94)	(0.21,0.33,0.92)	0.286°	1.985°
Fig. 5	(0.26,0.39,0.88)	(0.33,0.43,0.84)	(0.31,0.42,0.86)	5.452°	3.472°

5. CONCLUSION

In this paper, we present a non-diagonal model for color correction, which aimed to minimize the color bias while keeping the balance of white color in a tested image. The non-diagonal model provides more degrees of freedom and better color prediction. However, the challenge of using non-diagonal model to replace the diagonal model is more information is required in order to determine the optimal 3-by-3 transformation for color correction. In our system, we proposed to rely on the PCA-based learning process to gain extra information. By utilizing PCA to extract a compact subspace of illumination transformation matrix, we could record the mapping of environmental illumination and its optimal non-diagonal transformation. With the mapping model and the estimation of illumination, we can dynamically select the best matrix to correct the color biases and get a better white balance result.

Even though the learning process could provide information, the accuracy of the information is highly dependent on the training samples. Hence, we also proposed a sample selection method, which is specific designed for white balance algorithms.

In this paper, we find that we could have better color prediction through the learning process. In the future, we attempt to gain more information based on learning methods so that we could provide better color correction for the current white balance system. In addition, our future extension will also focus on the improvement of the accuracy.

6. REFERENCES

[1] K. Barnard, B. Funt, and V.Cardei, "A Comparison of Computational Color Constancy Algorithms, Part One: Theory and Experiments with Synthetic Data", *IEEE Transactions on Image Processing*, Vol. 11, No. 9, pp. 972-984, 2002.

[2] K. Barnard, B. Funt, and V.Cardei, "A Comparison of Computational Color Constancy Algorithms, Part two: Experiments with Images," *IEEE Transactions on Image Processing*, Vol. 11, No. 9, pp. 985-996, 2002.

[3] J. Weijer and Th. Gevers, "Color constancy based on the grey-edge hypothesis," *IEEE International Conference on Image Processing*, pp.722–725, Sept. 2005.

[4] B. Funt and H. Jiang, "Non-von-Kries 3-parameter Color Prediction," *in Proceeding of the SPIE Electronic Imaging Conference*, Vol. 5007, pp.182-189, 2003.

[5] S. D. Hordley and G. D. Finlayson, "Reevaluation of Color Constancy Algorithm Performance," *Journal of Optical Society of America A*, Vol. 23, No. 5, pp. 1008-1020, 2006.

[6] G.D. Finlayson, M. Drew and B. Funt, "Spectral Sharpening: Sensor Transformations for Improved Color Constancy," *Journal of Optical Society of America A*, Vol. 11, No. 5, pp. 1553-1563, 1994.

[7] Kobus Barnard, Florian Ciurea, and Brian Funt, "Sensor Sharpening for Computational Colour Constancy," *Journal of the Optical Society of America A*, Vol 18, No. 11, pp. 2728-2743, 2001.

[8] F. Xiao, J. Farrell, J. DiCarlo and B. Wandell, "Preferred Color Spaces for White Balancing," *in Proceedings of the SPIE Electronic Imaging Conference*, Vol. 5017, January 2003.

[9] K. Barnard, L. Martin, B. Funt and A. Coath, "A Data Set for Colour Research," *Color Research and Application*, Vol. 27, No. 3, pp. 147-151, 2002,

[10] G. Buchsbaum, "A spatial processor model for object color perception," *J. Franklin Inst.*, Vol. 310, pp. 1–26, 1980.

[11] G. Finlayson and E. Trezzi, "Shades of gray and colour constancy," in *Proc. IS&T/SID 12th Color Imaging Conference*, pp. 37–41, 2004.

[12] J. van de Weijer, Theo Gevers, and Arjan Gijsenij, "Edge-Based Color Constancy," *IEEE Transactions on Image Processing*, Vol. 16, No. 9, pp. 2207-2214, 2007.

[13] E.K.P. Chong and S.H. Zak, "An Introduction to Optimization," *John Wiley & Sons, Inc.* New York: 1996.